

Anisotropic, Fermi-Surface-Induced Variation in T_c in MgB_2 Alloys

Prabhakar P. Singh

Department of Physics, Indian Institute of Technology, Powai, Mumbai- 400076, India

(November 6, 2018)

Using coherent-potential to describe disorder, Gaspari-Gyorffy approach to evaluate electron-phonon coupling, and Allen-Dynes equation to calculate T_c , we show that in $Mg_{1-x}M_xB_2$ ($M \equiv Al, Li$ or Zn) alloys (i) the way T_c changes depends on the location of the added/modified \mathbf{k} -resolved states on the Fermi surface and (ii) the variation of T_c as a function of concentration is dictated by the B p DOS. In addition, using full-potential calculations for $MgMB_4$, we show that (i) at $x = 0.5$ a superstructure can form in $Mg_{1-x}Al_xB_2$ but not in $Mg_{1-x}Li_xB_2$ or $Mg_{1-x}Zn_xB_2$, and (ii) B layer shifts towards the impurity layer, more for Al than for Li or Zn .

PACS numbers: 74.25.Jb, 74.70.Ad

Since the discovery of superconductivity in MgB_2 [1] the experimental [1–6] and theoretical [7–16] efforts have greatly improved our understanding of the nature of interaction responsible for superconductivity (SC) in MgB_2 . It has become clear that almost all facets of the phonon-mediated electron-electron interaction have a dramatic influence over the superconducting behavior of MgB_2 . For example, the electron-phonon matrix elements change considerably as one moves away from the cylindrical Fermi sheets along Γ to A [9,16], anharmonic effects [6,15] have to be included in the dynamical matrix [16], and finally \mathbf{k} -dependent fully anisotropic Eliashberg equations have to be solved [16] for a complete and accurate description of the superconducting properties of MgB_2 . Such a strong dependence of the superconducting properties of MgB_2 on different aspects of the interaction has opened up the possibility of dramatically modifying its superconducting behavior by changing the interaction in various ways and thereby learning more about the interaction itself. Alloying MgB_2 with various elements and then studying their SC properties offers such an opportunity.

There have been several studies of changes in the SC properties of MgB_2 upon substitutions of various elements such as $Be, Li, C, Al, Na, Zn, Zr, Fe, Co, Ni$, and others [5,17–20]. The main effects of alloying are seen to be (i) a decrease in transition temperature, T_c , with increasing concentration of the alloying elements although the rate at which the T_c changes depends on the element being substituted, (ii) a slight increase in the T_c in case of Zn [19,20] substitution while for Si and Li the T_c remains essentially the same, (iii) persistence of superconductivity up to $x \sim 0.7$ in $Mg_{1-x}Al_xB_2$ [5,17], (iv) a change in crystal structure and the formation of a superstructure at $x = 0.5$ in $Mg_{1-x}Al_xB_2$ [17], and (v) a change in the lattice parameters a and c .

In an effort to understand the changes in the electronic structure and the superconducting properties of MgB_2 alloys, we have carried out *ab initio* studies of $Mg_{1-x}Al_xB_2$, $Mg_{1-x}Li_xB_2$ and $Mg_{1-x}Zn_xB_2$ al-

loys. We have used Korringa-Kohn-Rostoker coherent-potential approximation [21,22] in the atomic-sphere approximation (KKR-ASA CPA) method for taking into account the effects of disorder, Gaspari-Gyorffy formalism [23] for calculating the electron-phonon coupling constant λ , and Allen-Dynes equation [24] for calculating T_c in $Mg_{1-x}Al_xB_2$, $Mg_{1-x}Li_xB_2$ and $Mg_{1-x}Zn_xB_2$ alloys as a function of Al , Li and Zn concentrations, respectively. We have analyzed our results in terms of the changes in the spectral function [22] along Γ to A evaluated at the Fermi energy, E_F , and the total density of states (DOS), in particular the changes in the B p contribution to the total DOS, as a function of concentration x .

For examining the possibility of superstructure formation at $x = 0.5$, we have used ABINIT code [25], based on pseudopotentials and plane waves to optimize the cell parameters a and c as well as relax the cell-internal atomic positions of $MgAlB_4$, $MgLiB_4$ and $MgZnB_4$ in $P6/mmm$ structures. We have used these atomic positions to carry out a total energy comparison using KKR-ASA CPA between the ordered and the substitutionally disordered $Mg_{1-x}Al_xB_2$, $Mg_{1-x}Li_xB_2$ and $Mg_{1-x}Zn_xB_2$ alloys at $x = 0.5$. Such an approach allows us to check the possibility of formation of a layered or a mixed superstructure at $x = 0.5$ in these alloys. Before we describe our results, we outline some of the computational details.

The charge self-consistent electronic structure of $Mg_{1-x}Al_xB_2$, $Mg_{1-x}Li_xB_2$ and $Mg_{1-x}Zn_xB_2$ alloys as a function of x has been calculated using the KKR-ASA CPA method. We have used the CPA rather than a rigid-band model because CPA has been found to reliably describe the effects of disorder in metallic alloys [21,22]. We parametrized the exchange-correlation potential as suggested by Perdew-Wang [26] within the generalized gradient approximation. The Brillouin zone (BZ) integration was carried out using 1215 k -points in the irreducible part of the BZ. For DOS and spectral function calculations, we added a small imaginary component of 1 mRy and 2 mRy , respectively, to the energy

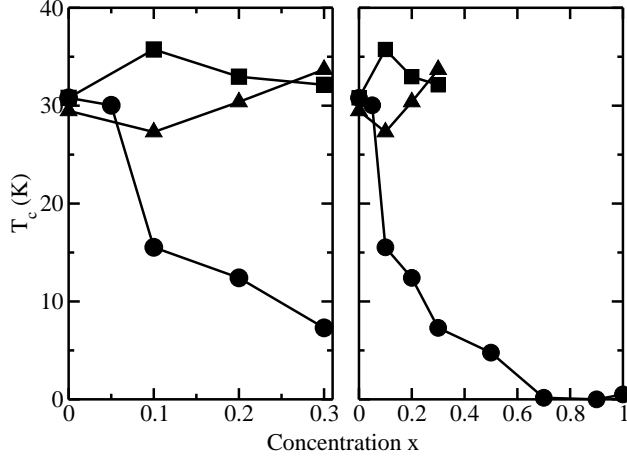


FIG. 1. The calculated variation of T_c as a function of concentration x in $Mg_{1-x}Al_xB_2$, $Mg_{1-x}Li_xB_2$ and $Mg_{1-x}Zn_xB_2$ alloys.

and used 4900 \mathbf{k} -points in the irreducible part of the BZ. The lattice constants for $Mg_{1-x}Al_xB_2$, $Mg_{1-x}Li_xB_2$ and $Mg_{1-x}Zn_xB_2$ alloys as a function of x were taken from experiments [17–19]. The Wigner-Seitz radii for Mg , Al and Zn were slightly larger than that of B . The sphere overlap which is crucial in ASA, was less than 10% and the maximum l used was $l_{max} = 3$.

The electron-phonon coupling constant λ was calculated using Gaspari-Gyorffy [23] formalism with the charge self-consistent potentials of $Mg_{1-x}Al_xB_2$, $Mg_{1-x}Li_xB_2$ and $Mg_{1-x}Zn_xB_2$ obtained with the KKR-ASA CPA method. Subsequently, the variation of T_c as a function of Al , Li and Zn concentrations was calculated using Allen-Dynes equation [24]. The average values of phonon frequencies ω_{ln} for MgB_2 and AlB_2 were taken from Refs. [9,10] respectively. For intermediate concentrations, we took ω_{ln} to be the concentration-weighted average of MgB_2 and AlB_2 . For $Mg_{1-x}Li_xB_2$ and $Mg_{1-x}Zn_xB_2$ we used the same value of ω_{ln} as that for MgB_2 .

The structural relaxation of $MgAlB_4$, $MgLiB_4$ and $MgZnB_4$ was carried out by the molecular dynamics program ABINIT with Broyden-Fletcher-Goldfarb-Shanno minimization technique [25] using Troullier-Martins pseudopotentials [27], 512 Monkhorst-Pack [28] \mathbf{k} -points and Teter parameterization [25] for exchange-correlation. The kinetic energy cutoff for the plane waves was 110 Ry.

Based on our calculations, described below, we find that in $Mg_{1-x}Al_xB_2$, $Mg_{1-x}Li_xB_2$ and $Mg_{1-x}Zn_xB_2$ alloys (i) the way T_c changes depends on the location of the added/modified \mathbf{k} -resolved states on the Fermi surface, (ii) the variation of T_c as a function of concentration

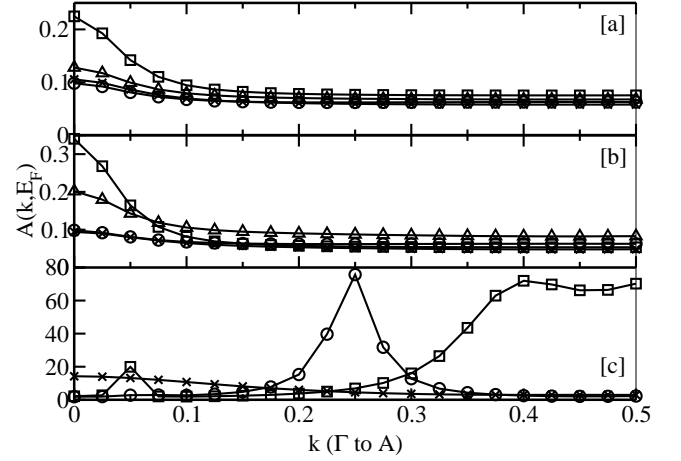


FIG. 2. The calculated spectral function along Γ to A , evaluated at the Fermi energy, as a function of concentration x in $Mg_{1-x}Al_xB_2$, $Mg_{1-x}Li_xB_2$ and $Mg_{1-x}Zn_xB_2$ alloys. Figures (a) and (b) correspond to $x = 0.1$ and $x = 0.3$, respectively and the symbols open circle, open square, x and open triangle correspond to MgB_2 , $Mg_{1-x}Al_xB_2$, $Mg_{1-x}Li_xB_2$ and $Mg_{1-x}Zn_xB_2$ alloys respectively. In figure (c) the symbols open circle, open square and x correspond to AlB_2 , $Mg_{0.1}Al_{0.9}B_2$ and $Mg_{0.4}Al_{0.6}B_2$, respectively. For clarity, in figure (c) we have multiplied the spectral function of $Mg_{0.4}Al_{0.6}B_2$ by 100.

is dictated by the Bp contribution to the total DOS, (iii) at $x = 0.5$ a superstructure can form in $Mg_{1-x}Al_xB_2$ but not in $Mg_{1-x}Li_xB_2$ or $Mg_{1-x}Zn_xB_2$, and (iv) B layer shifts towards the impurity layer, more for Al than for Li or Zn .

The main results of our calculations are shown in Fig. 1, where we have plotted the variation in T_c of $Mg_{1-x}Al_xB_2$, $Mg_{1-x}Li_xB_2$ and $Mg_{1-x}Zn_xB_2$ alloys as a function of concentration x . The calculations were carried out as described earlier with the same value of $\mu^* = 0.09$ for all the concentrations. The T_c for MgB_2 is equal to ~ 30.8 K, which is consistent with the results of other works [7,9,10] with similar approximations. The corresponding λ is equal to 0.69. For $0 < x \leq 0.3$, the T_c increases slightly for $Mg_{1-x}Li_xB_2$ and $Mg_{1-x}Zn_xB_2$, while it decreases substantially for $Mg_{1-x}Al_xB_2$, as is found experimentally [5,17]. Note that for $x = 0.1$, our calculation shows $Mg_{1-x}Li_xB_2$ to have a T_c higher than that of $Mg_{1-x}Zn_xB_2$ by about 7 K [18–20]. In Fig.1 (right panel) we have shown the variation in T_c in $Mg_{1-x}Al_xB_2$ alloys as a function of concentration for $0 \leq x \leq 1$. As a function of Al concentration, the T_c decrease rapidly from 30 K at $x = 0.05$ to about 15 K at $x = 0.1$. The T_c decreases slowly between $x = 0.4$ and $x = 0.5$. At $x = 0.7$ the T_c vanishes and remains essen-

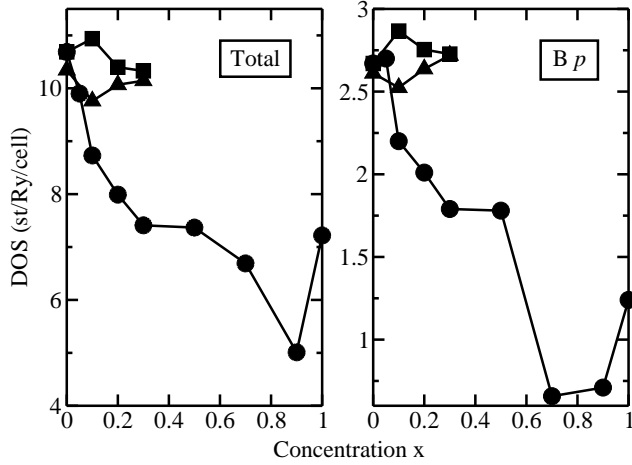


FIG. 3. The calculated total density of states at the Fermi energy (left panel) and the $B p$ contribution to the total DOS (right panel) in $Mg_{1-x}Al_xB_2$, $Mg_{1-x}Li_xB_2$ and $Mg_{1-x}Zn_xB_2$ alloys.

tially zero thereafter. The calculated variation in T_c , as shown in Fig. 1, is in very good qualitative agreement with the experiments [5].

In order to understand the variation of T_c in $Mg_{1-x}Al_xB_2$, $Mg_{1-x}Li_xB_2$ and $Mg_{1-x}Zn_xB_2$ alloys as a function of concentration x , we have analyzed our results in terms of the spectral functions, the contribution of Boron p -electrons to the total DOS and the total DOS. In Fig. 2(a)-(c), we show the spectral functions along Γ to A direction evaluated at E_F in $Mg_{1-x}Al_xB_2$, $Mg_{1-x}Li_xB_2$ and $Mg_{1-x}Zn_xB_2$ alloys for $x = 0.1$ (Fig. 2(a)), $x = 0.3$ (Fig. 2(b)), and $x = 0.6 - 1.0$ (Fig. 2(c)). From Figs. 2(a)-(b) it is clear that the substitution of Al in MgB_2 leads to creation of more new states along Γ to A direction than the substitution of Zn or Li . Since the hole-like cylindrical Fermi sheet along Γ to A contributes much more to the electron-phonon coupling [16], the creation of new electron states along Γ to A direction weakens considerably the overall coupling constant λ , which, in turn, reduces the T_c more in $Mg_{1-x}Al_xB_2$ than in either $Mg_{1-x}Zn_xB_2$ or $Mg_{1-x}Li_xB_2$. Thus, in our opinion, the way T_c changes in MgB_2 upon alloying depends dramatically on the location of the added/modified \mathbf{k} -resolved states on the Fermi surface.

Having explained the differences in behavior of MgB_2 upon alloying with Al , Li and Zn , we now try to understand the changes in their properties as a function of concentration x . In Fig. 3(a)-(b) we have shown the total DOS at E_F (Fig. 3(a)) and the $B p$ contribution to the total DOS at E_F (Fig. 3(b)) in $Mg_{1-x}Al_xB_2$, $Mg_{1-x}Li_xB_2$ and $Mg_{1-x}Zn_xB_2$ alloys as a function of concentration x . We find that as a function of concentra-

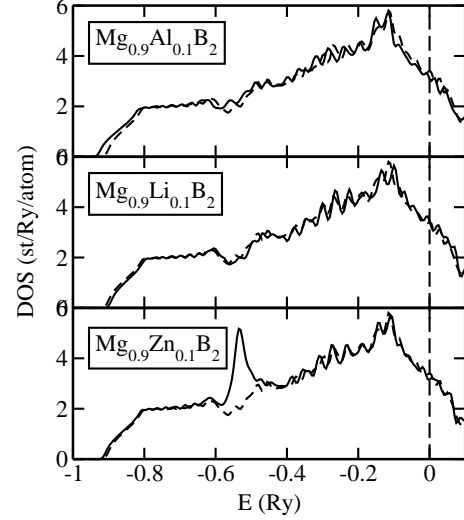


FIG. 4. The calculated total density of states (solid line) for $Mg_{0.9}Al_{0.1}B_2$ (upper panel), $Mg_{0.9}Li_{0.1}B_2$ (middle panel) and $Mg_{0.9}Zn_{0.1}B_2$ (lower panel) alloys. For comparison the total DOS for MgB_2 (dashed line) is also shown. The dashed vertical line indicates the Fermi energy.

tion, the variation in T_c , as shown in Fig. 1, follows closely the behavior of the total DOS at E_F and in particular the variation in $B p$ contribution to the total DOS at E_F . It is also not surprising to see that the vanishing of superconductivity in $Mg_{1-x}Al_xB_2$ at $x \sim 0.7$ coincides with a very small $B p$ contribution to the total DOS.

In Fig. 4(a)-(c) we show the total DOS of $Mg_{1-x}Al_xB_2$, $Mg_{1-x}Li_xB_2$ and $Mg_{1-x}Zn_xB_2$ alloys, respectively, at $x = 0.1$. In the same plot we also show the total DOS of MgB_2 obtained using the same approach. The overall downward (upward) movement of the total DOS in $Mg_{0.9}Al_{0.1}B_2$ ($Mg_{0.9}Li_{0.1}B_2$) with respect to that of MgB_2 is due to the addition (removal) of electrons. In Fig. 4(c), the peak in the total DOS at around $0.53 Ry$ below E_F is due to the $3d$ states of Zn .

Finally, we discuss the possibility of superstructure formation at $x = 0.5$. In Table I we show the optimized cell parameters as well as the cell-internal relaxations for $MgAlB_4$, $MgLiB_4$ and $MgZnB_4$ calculated using the ABINIT program. We find that the Boron layer shifts significantly more towards Al layer in $MgAlB_4$ than towards either Li or Zn layer in $MgLiB_4$ or $MgZnB_4$, respectively. The shift of B layer by $\sim 0.24 a.u.$ towards Al layer in $MgAlB_4$ compares well with the corresponding shift obtained in Ref. [29]. However, the shift of B layer towards Li and Zn layers in $MgLiB_4$ and $MgZnB_4$ respectively implies that it is not simply due to the extra positive charge on the impurity layer, as suggested in Ref. [29] in the case of $MgAlB_4$. In Table I we have also listed the calculated ordering energy, E_{ord} , which is the difference between the total energies of the

TABLE I. The calculated lattice constants a and c/a , the shift δ of the B layer along the c -axis towards the impurity layer, and the ordering energy E_{ord} at $x = 0.5$. The lattice constant a and the shift δ are in atomic units while E_{ord} is in $mRy/atom$.

Alloy	a	c/a	δ	E_{ord}
$MgAlB_4$	5.799	2.242	0.24	-12.1
$MgLiB_4$	5.685	2.287	0.04	+4.8
$MgZnB_4$	5.789	2.254	0.08	+1.2

ordered $MgAlB_4$, $MgLiB_4$ and $MgZnB_4$ and the corresponding disordered $Mg_{0.5}Al_{0.5}B_2$, $Mg_{0.5}Li_{0.5}B_2$ and $Mg_{0.5}Zn_{0.5}B_2$ alloys, obtained using KKR-ASA CPA method. It clearly shows the possibility of formation of a superstructure in $Mg_{0.5}Al_{0.5}B_2$ because the fully-relaxed $MgAlB_4$ is lower in energy by 12 $mRy/atom$ in comparison to the disordered $Mg_{0.5}Al_{0.5}B_2$. However, within the limitations of our approach, we find that $Mg_{0.5}Li_{0.5}B_2$ and $Mg_{0.5}Zn_{0.5}B_2$ are unlikely to form superstructures since E_{ord} is positive in these two cases. Our results also show that a structure made up of layers consisting of a random mixing of Mg and Al atoms and described by CPA, is higher in energy than a structure made up of alternate layers of Mg and Al atoms [29].

In conclusion, we have shown that in $Mg_{1-x}Al_xB_2$, $Mg_{1-x}Li_xB_2$ and $Mg_{1-x}Zn_xB_2$ alloys (i) the way T_c changes depends on the location of the added/modified \mathbf{k} -resolved states on the Fermi surface, (ii) the variation of T_c as a function of concentration is dictated by the Bp contribution to the total DOS at E_F , (iii) at $x = 0.5$ a superstructure can form in $Mg_{1-x}Al_xB_2$ but not in $Mg_{1-x}Li_xB_2$ or $Mg_{1-x}Zn_xB_2$, and (iv) B layer shifts towards the impurity layer, more for Al than for Li or Zn .

[1] J. Nagamatsu *et al.*, Nature, **410**, 63 (2001).
[2] S. L. Bud'ko *et al.*, Phys. Rev. Lett. **86**, 1877 (2001).
[3] D. G. Hinks *et al.*, Nature **411**, 457 (2001).
[4] T. Takahashi *et al.*, Phys. Rev. Lett. **86**, 4915 (2001).
[5] Cristina Buzea and Tsutomu Yamashita, cond-mat/0108265; and references therein.
[6] T. Yildirim *et al.*, Phys. Rev. Lett. **86**, 5771 (2001).
[7] J. Kortus *et al.*, Phys. Rev. Lett. **86**, 4656 (2001).
[8] M. An and W. E. Pickett, Phys. Rev. Lett. **86**, 4366 (2001).
[9] Y. Kong *et al.*, Phys. Rev. B **64**, 020501 (2001).
[10] K.-P. Bohnen *et al.*, Phys. Rev. Lett. **86**, 5771 (2001).
[11] Prabhakar P. Singh Phys. Rev. Lett. **87**, 087004 (2001).
[12] N. I. Medvedeva *et al.*, Phys. Rev. B **64**, 020502 (2001).
[13] G. Satta *et al.*, Phys. Rev. B **64**, 104507 (2001).
[14] K. D. Belaschenko *et al.*, Phys. Rev. B **64**, 092503 (2001).

[15] A. Liu *et al.*, Phys. Rev. Lett. **87**, 87005 (2001).
[16] H. J. Choi *et al.*, cond-mat/0111182 and cond-mat/0111183 (2001).
[17] J. Y. Xiang *et al.*, cond-mat/0104366 (2001).
[18] Y. G. Zhang *et al.*, Phys. C **361**, 91 (2001).
[19] S. M. Kazakov *et al.*, cond-mat/0103350 (2001).
[20] Y. Moritomo *et al.*, cond-mat/0104568 (2001).
[21] Prabhakar P. Singh and A. Gonis, Phys. Rev. B **49**, 1642 (1994).
[22] J. S. Faulkner, Prog. Mat. Sci **27**, 1 (1982); and references therein.
[23] G. D. Gaspari and B. L. Gyorffy, Phys. Rev. Lett. **28**, 801 (1972).
[24] P. B. Allen and R. C. Dynes, Phys. Rev. B **12**, 905 (1975).
[25] See URL <http://www.pcpm.ucl.ac.be/abinit>.
[26] J. P. Perdew and Y. Wang, Phys. Rev. B **45**, 13244 (1992); J. Perdew *et al.*, Phys. Rev. Lett. **77**, 3865 (1996).
[27] N. Troullier and J. L. Martins, Phys. Rev. B **43**, 1993 (1991).
[28] H. J. Monkhorst and J. D. Pack, Phys. Rev. B **13**, 5188 (1976).
[29] S. V. Barabash *et al.*, cond-mat/0111392 (2001).